

Electronic Supplementary Information

**Origin and Mechanism Analysis of Asymmetric
Current Fluctuations in Single-Molecule Junctions**

*Chunhui Gu^{‡a}, Hao Wang^{‡b}, Hantao Sun^b, Jianhui Liao^b, Shimin Hou^{*b}, Xuefeng Guo^{*a}*

^a. Beijing National Laboratory for Molecular Sciences, State Key Laboratory for Structural Chemistry of Unstable and Stable Species, College of Chemistry and Molecular Engineering, Peking University, Beijing 100871, P. R. China.
Email: guoxf@pku.edu.cn

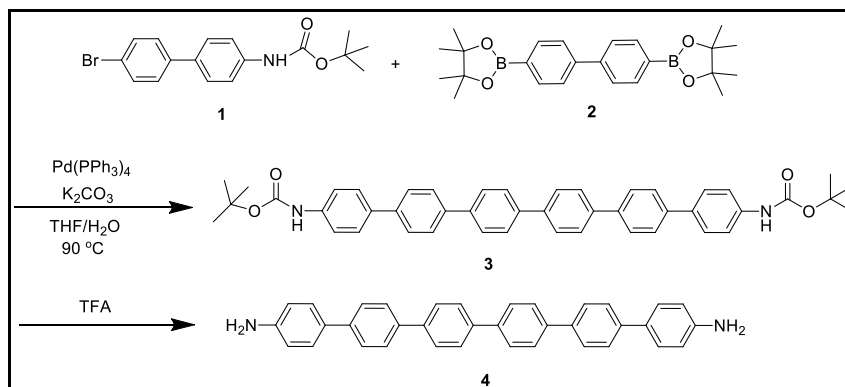
^b. Key Laboratory for the Physics and Chemistry of Nanodevices, Department of Electronics, Peking University, Beijing 100871, P. R. China.
Email: smhou@pku.edu.cn

[‡]These authors contributed equally to the work.

Table of Contents

1. Synthesis of a Hexaphenyl Molecule.....	S3
2. Device Fabrication and Characterization.....	S4
3. Current-Time ($I-t$) Profiles of Single-Molecule Devices.....	S7
4. The Fabrication of Graphene Nanoconstrictions.....	S11
5. Current-Time ($I-t$) Profiles of Graphene Nanoconstrictions.....	S12
6. The Current, Standard Deviation and Skewness of Different Types of Single-Molecule Devices.....	S13
7. Theoretical Calculations.....	S15
8. Reference.....	S25

1. Synthesis of a Hexaphenyl Molecule:



Scheme S1. Synthesis of a Hexaphenyl Molecule.

To a three-necked schlenk flask (150 mL) were added **1** (1.04 g, 3 mmol), **2** (0.41 g, 1 mmol), K_2CO_3 (1.80 g, 13.0 mmol), and $\text{Pd(PPh}_3)_4$ (58 mg, 0.05 mmol). The flask was evacuated and back-filled with argon atmosphere over three times, after which a degassed THF/ H_2O co-solvent (15 mL/7 mL) were injected into the flask through syringe. The mixture was heated up to 90°C and stirred for 14 h. After cooling to room temperature, the reaction mixture was poured into water, and then extracted with CH_2Cl_2 . The organic layer was dried over anhydrous MgSO_4 and filtered off from an insoluble fraction. The solvent was removed under reduced pressure. Then the crude product was purified by silica gel column chromatography (eluent, petroleum ether: ethyl acetate = 9:1) to give compound **3** as a light yellow powder. This solid was then dissolved in a mixture of CH_2Cl_2 (3 mL) and TFA (3 mL) and stirred for 2 h at room temperature. The solvent was removed under vacuum to give the target compound **4** (0.37g, 75%) as a light yellow powder. ^1H NMR (d_6 -DMSO, 400 MHz, ppm) δ 7.99-7.60 (m, 16H), 7.47 (d, J = 7.4 Hz, 4H), 6.67 (d, J = 6.7 Hz, 4H), 5.28 (s, 4H). HR-MS (MALDI-TOF, m/z): calcd. For $\text{C}_{36}\text{H}_{28}\text{N}_2$: 488.2252 [M^+]; Found: 488.0872.

2. Device Fabrication and Characterization:

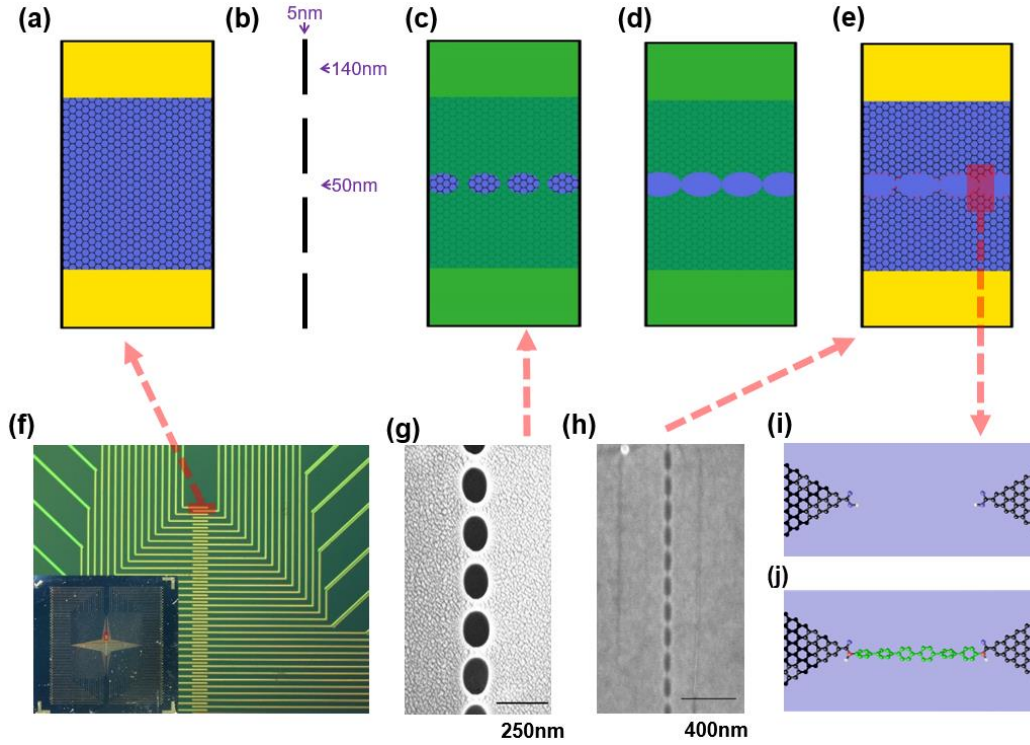


Figure S1. The fabrication of single-molecule devices. (a-e) Schematic of the fabrication process of graphene point contact electrode arrays. (f) Optical image of electrode arrays on graphene sheets. The inset shows the picture of a whole device. (g) SEM image of a representative dash-line window array on a PMMA mask (Gold sprayed). (h) SEM image of a representative graphene point contact electrode array. (i) Schematic of a point contact nanoelectrode unit. (j) Schematic of a SMJ based on graphene point contacts.

The ratio of single-junction devices to the overall reconnected devices is evaluated by statistics based on a binomial distribution reported before.¹ Particularly, the probability of the connected devices with n -rejoined junctions (G_n) can be calculated from a binomial distribution in the following equation, where m is the number of graphene point contact pairs (210 in this case), p is the connection success rate for each pair.

$$G_n = \frac{m!}{n!(m-n)!} p^n (1-p)^{m-n} \quad n=0,1,2 \dots, m$$

$$Y_{\text{connection}} = 1 - G_0 = 1 - \frac{m!}{0!(m-0)!} p^0 (1-p)^m$$

The optimized connection yield ($Y_{\text{connection}}$) equals to $1 - G_0$, where G_0 is the probability of devices without any connection. The optimized connection yield ($Y_{\text{connection}}$) was ~15%. In combination with the following equations, the probability of

the connected device with a single junction is $\sim 92\%$. That means, in most cases, charge transport in these devices mainly exists in a single-molecule junction.

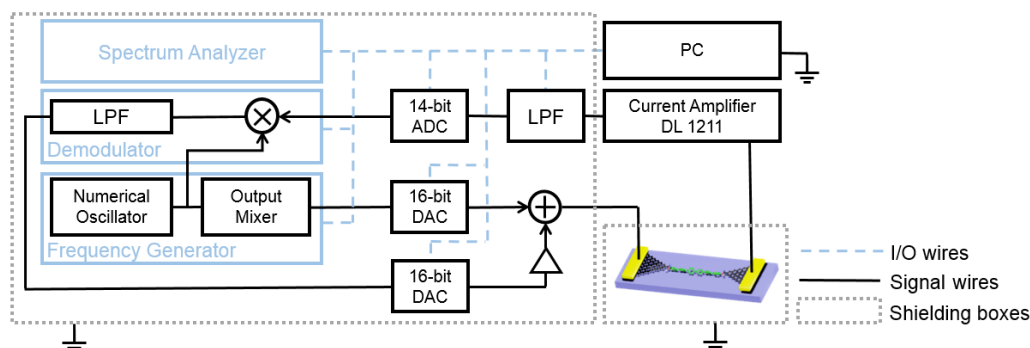


Figure S2. The real-time measurement apparatus

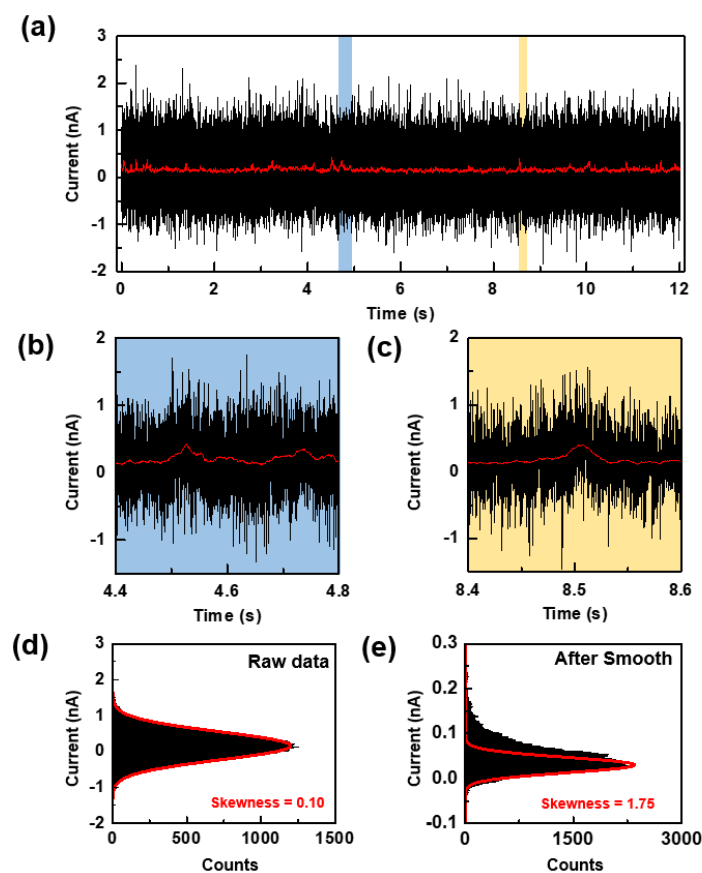


Figure S3. Time-varying mean computation. a) A representative $I-t$ profile of a single-molecule device. Black and red line show the raw data and smoothed data respectively. b,c) The enlarged scale of blue/orange area in (a), respectively. d,e) The distribution histograms of raw data (black) and smoothed data (red) in (a), respectively. The red line is fitted in Gaussian function according to the steep side of the histogram, aiming to highlight the asymmetric tail. The skewness value changes from 0.10 to 1.75 after smoothing.

A recurrence average filter was carried on via a Matlab 2009a software. The average number was set as 250. Figure S3a shows a representative $I-t$ trajectory before (black) and after (red) the recurrence average filter and Figures S3d and S3e show the corresponding current distributions. The skewness of both current distributions was calculated to be 0.10 and 1.75, respectively. Collectively, such results show that the recurrence average filter effectively protrudes the asymmetric factors in the current distribution.

3. Current-Time ($I-t$) Profiles of Single-Molecule Devices:

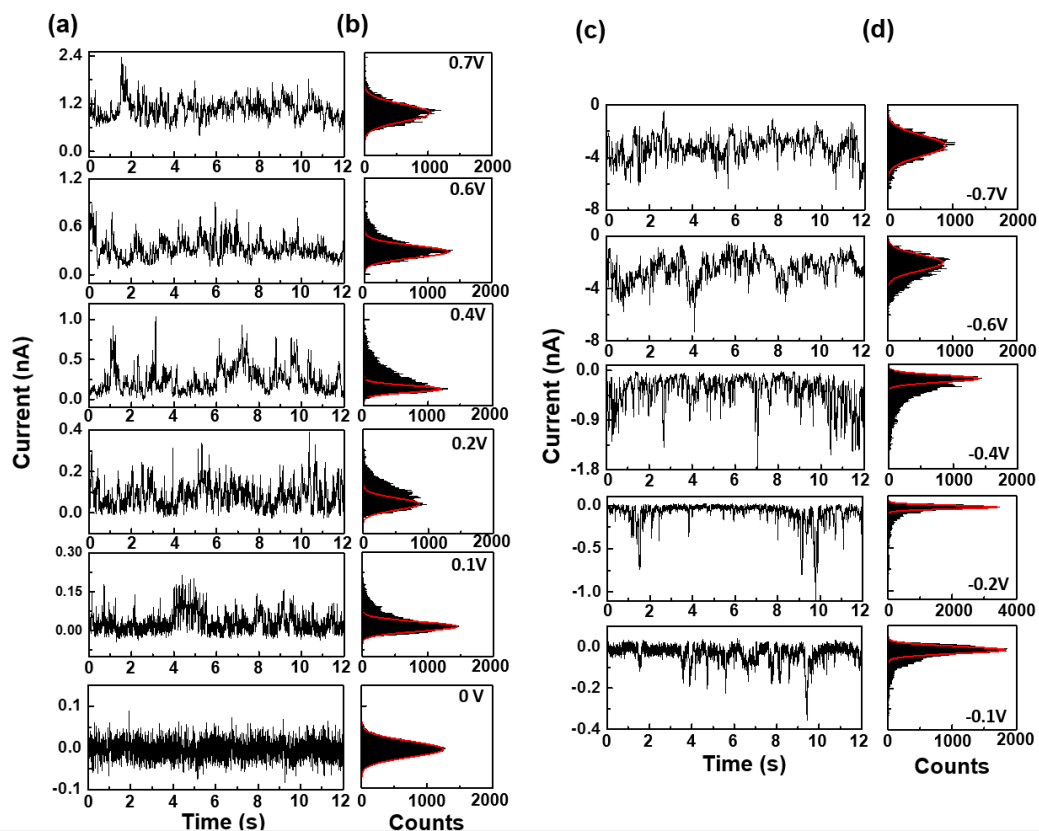


Figure S4. (a,c) $I-t$ profiles of Device 2 at representative bias voltages. (b,d) The corresponding distribution histograms. The red line is fitted in Gaussian function according to the steep side of the histogram, aiming to highlight the asymmetric tail.

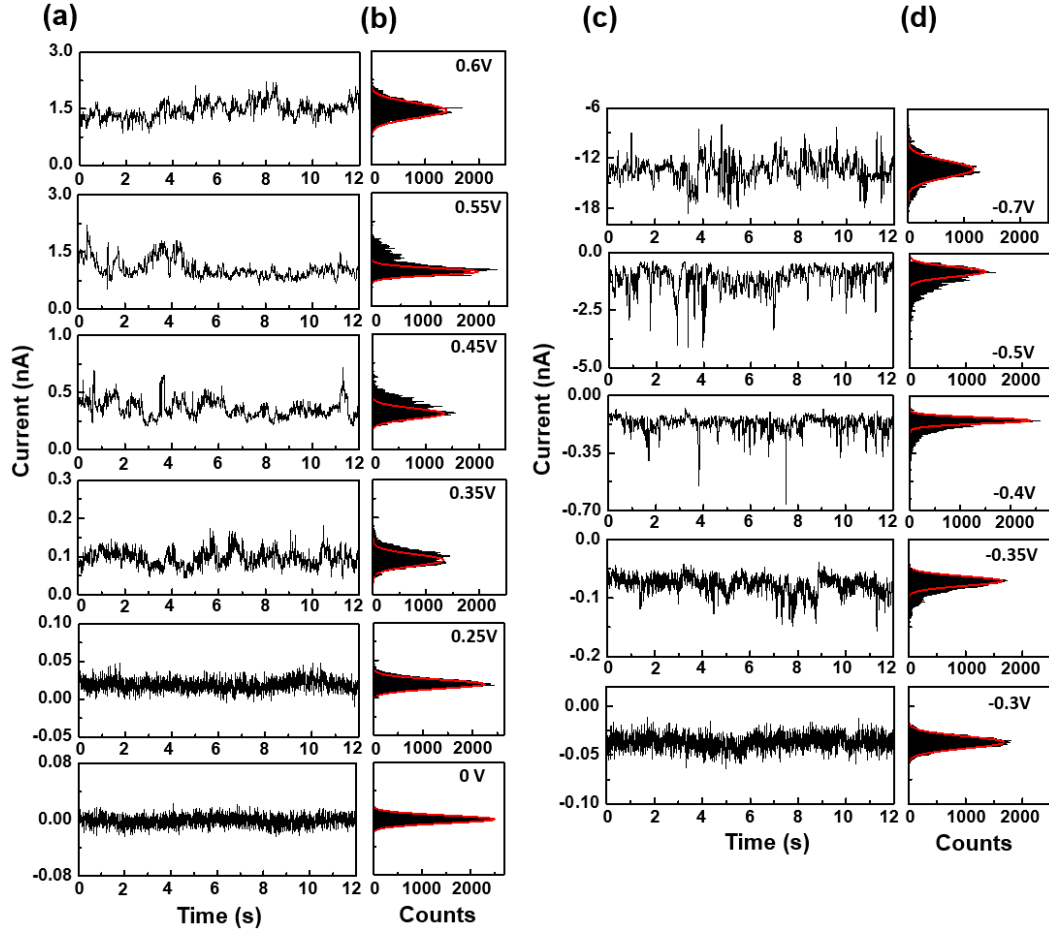


Figure S5. (a,c) $I-t$ profiles of Device 3 at representative bias voltages. (b,d) The corresponding distribution histograms. The red line is fitted in Gaussian function according to the steep side of the histogram, aiming to emphasis the asymmetric tail.

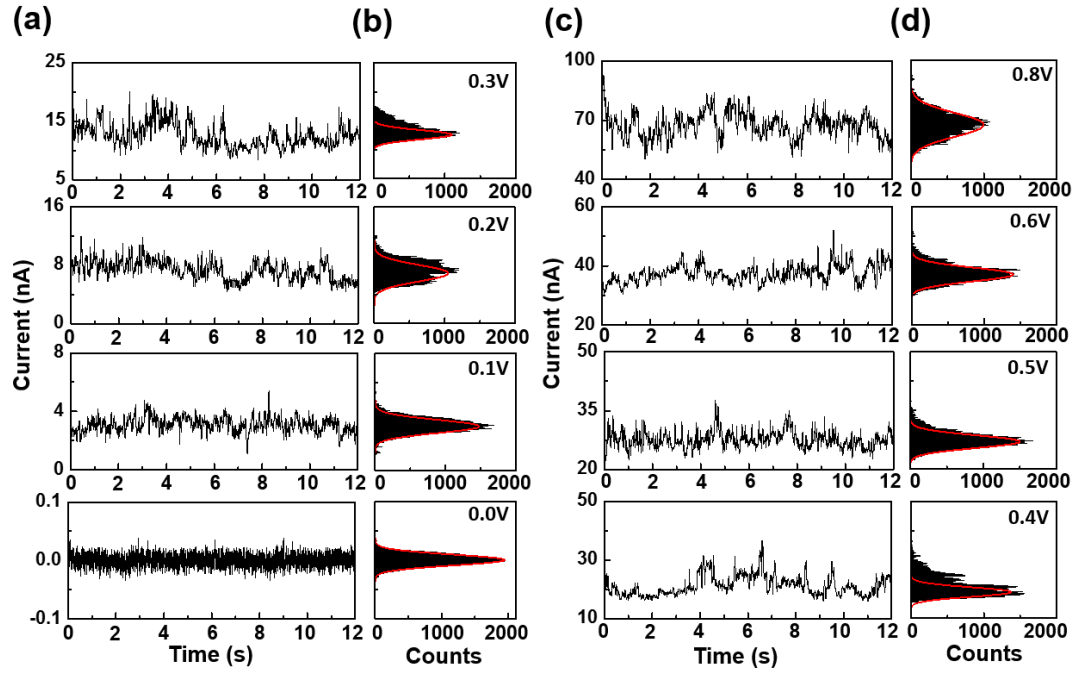


Figure S6. (a,c) $I-t$ profiles of Device 4 at representative bias voltages. (b,d) The corresponding distribution histograms. The red line is fitted in Gaussian function according to the steep side of the histogram, aiming to emphasis the asymmetric tail.

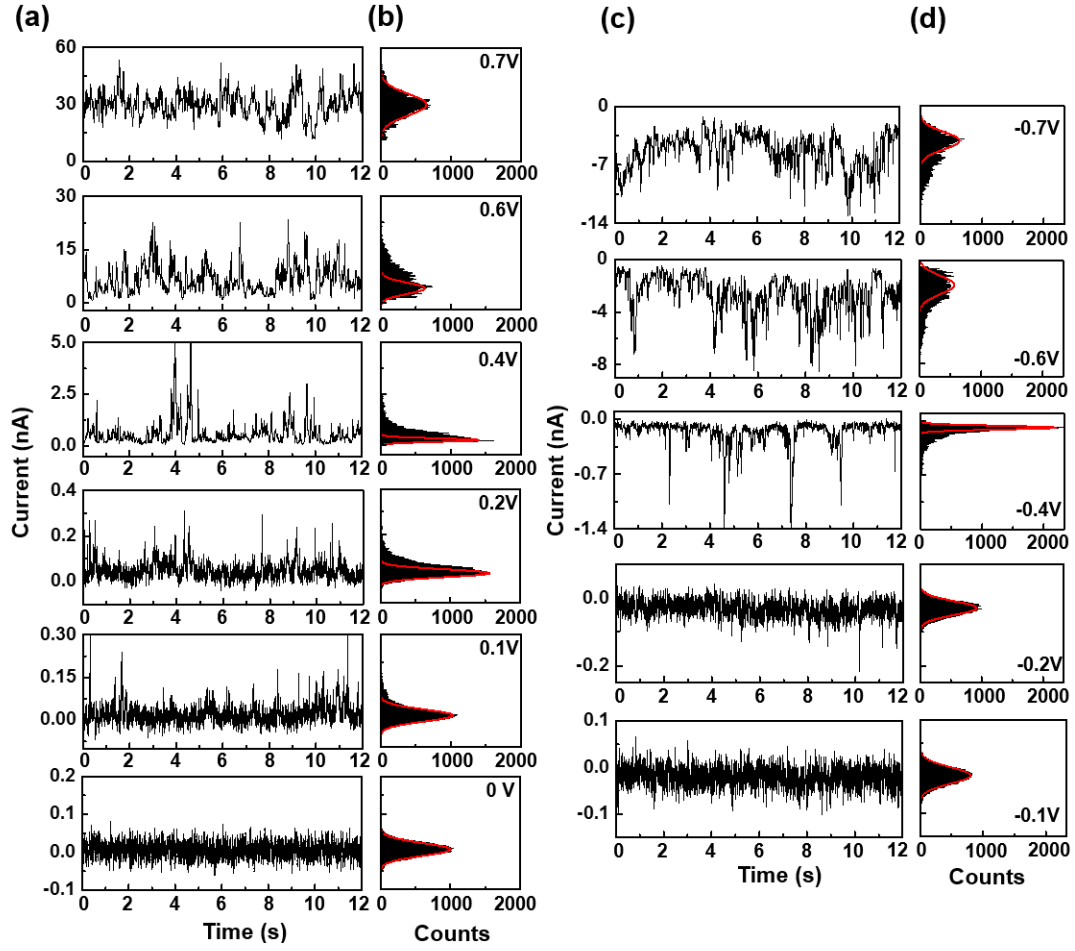


Figure S7. (a,c) $I-t$ profiles of Device 5 at representative bias voltages. (b,d) The corresponding distribution histograms. The red line is fitted in Gaussian function according to the steep side of the histogram, aiming to emphasis the asymmetric tail.

4. The Fabrication of Graphene Nanoconstrictions:

The graphene nanoconstriction was fabricated via precisely controlled oxygen plasma cutting technology referred in Section 1 in the Supporting Information. The plasma dose is precisely controlled to etch a narrow graphene homojunction rather than cut the graphene off.

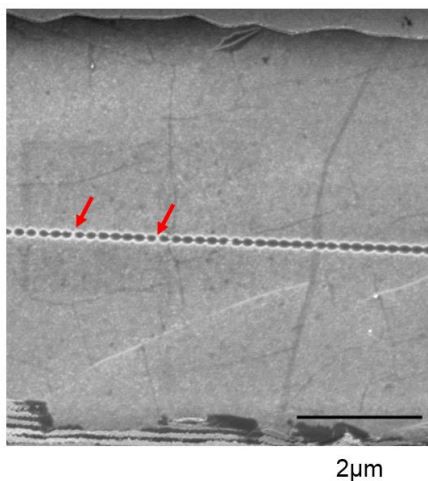


Figure S8. A typical SEM picture of graphene nanoconstrictions. The red arrows show the uncut-off part of the graphene

5. Current-Time ($I-t$) Profiles of Graphene Nanoconstrictions

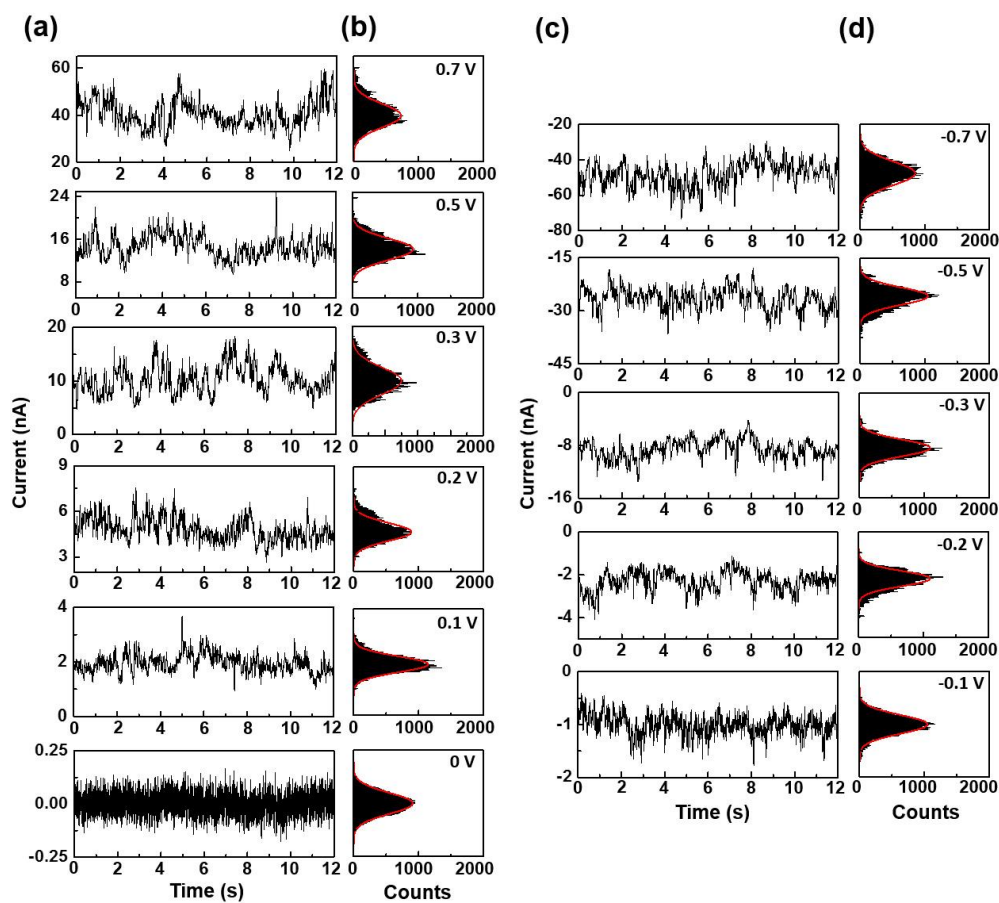


Figure S9. (a,c) $I-t$ profiles of a graphene nanoconstriction at representative bias voltages. (b,d) The corresponding distribution histograms. The red line is fitted in Gaussian function according to the steep side of the histogram, aiming to emphasis the asymmetric tail.

6. The Current, Standard Deviation and Skewness of Different Types of Single-Molecule Devices:

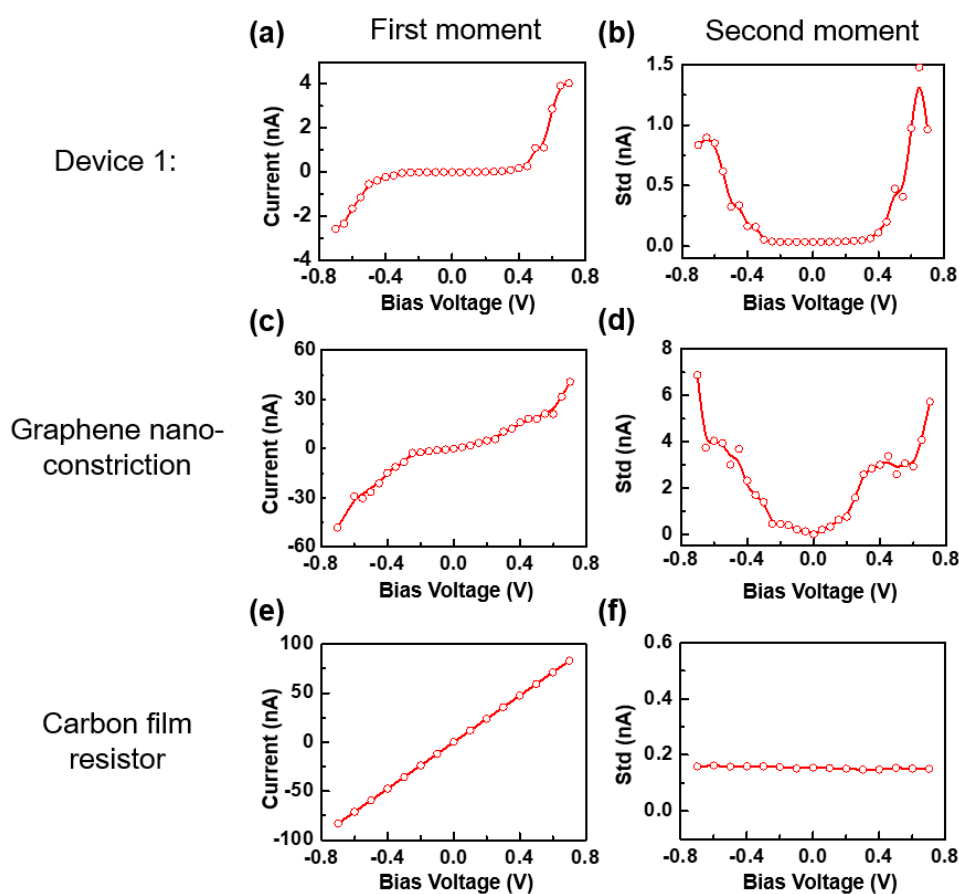


Figure S10. (a,c,e) The I - V characteristics of a single-molecule device (Device 1) in the main text, a graphene nanoconstriction, and a carbon film resistor, respectively. (b,d,f) The standard deviation (Std) of the current distribution of Device 1, a graphene nanoconstriction, and a carbon film resistor, respectively.

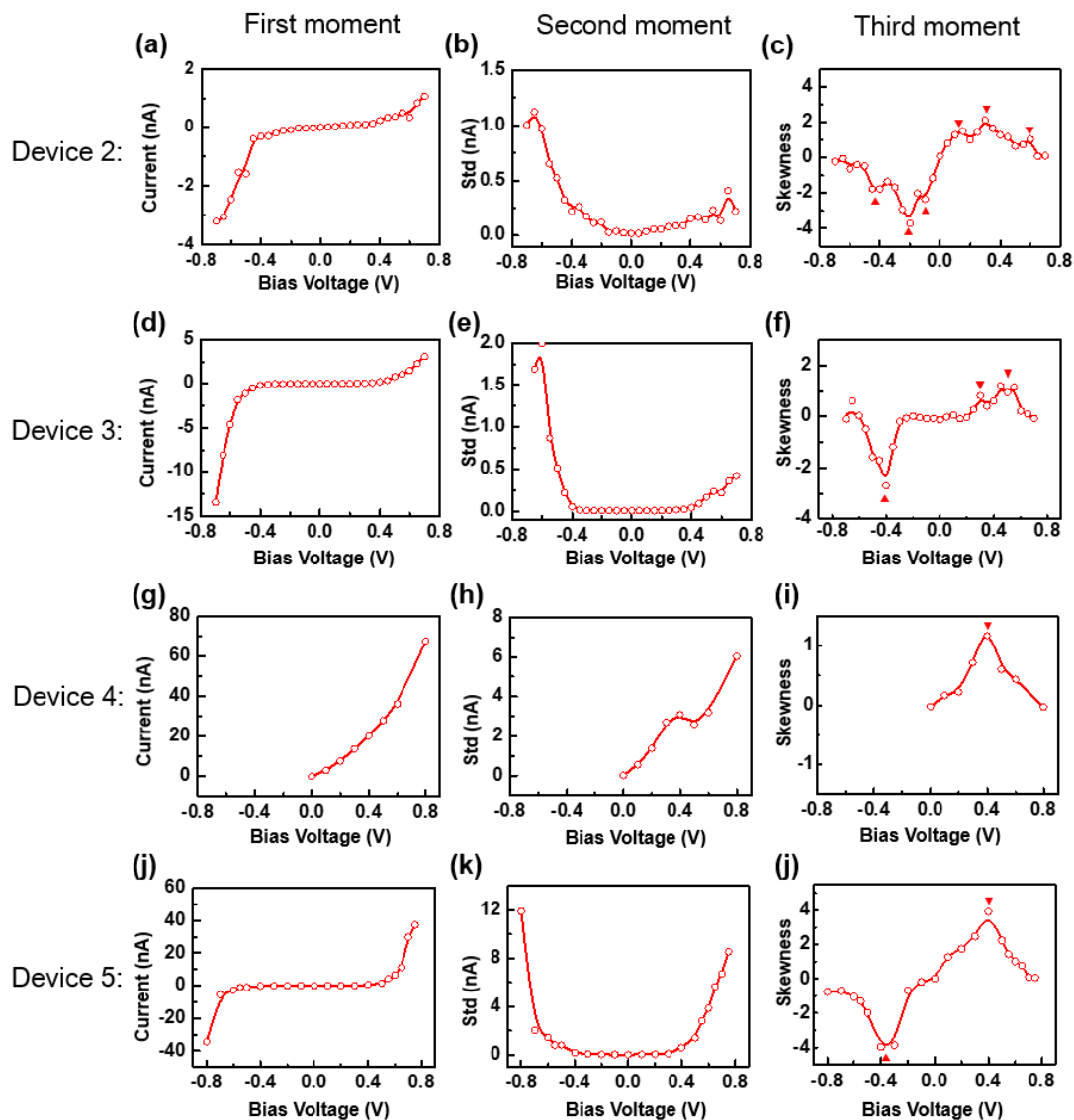


Figure S11. The I - V characterization (a,d,g,k), standard deviation (Std) of the current distribution (b,e,h,l) and skewness of the current distribution (c,f,j,m) of single-molecule devices (Devices 2–5), respectively.

7. Theoretical Calculations:

The full counting statistics allows us to address the current cumulants to any desired order. A single-level model was used in this approach:

(i) The skewness is defined as

$$\frac{A_{el} + A_H + A_F}{(S_{el} + S_H^{mf} + S_H^{vx} + S_F^{mf} + S_F^{vx})^{\frac{3}{2}}} \quad (1)$$

where A_{el} , A_H , and A_F represent the elastic term, the Hartree term and the Fock term of the 3rd cumulant A , respectively; S_{el} , S_H , and S_F represent the elastic term, the Hartree term and the Fock term of the 2nd cumulant S , respectively. The superscripts mf and vx refer to the mean-field and the vertex corrections, respectively.

(ii) The elastic terms of the 2nd cumulant S and the 3rd cumulant A are expressed as:

$$\begin{aligned} S_{el} &= e^2 \int \frac{d\varepsilon}{2\pi\hbar} T(\varepsilon) (1-T(\varepsilon)) (f_L(\varepsilon) \bar{f}_R(\varepsilon) + \bar{f}_L(\varepsilon) f_R(\varepsilon)) + [T(\varepsilon)]^2 (f_L(\varepsilon) \bar{f}_L(\varepsilon) + \bar{f}_R(\varepsilon) f_R(\varepsilon)) \\ &= \frac{e^2}{h} \left\{ T(\varepsilon) (1-T(\varepsilon)) eV \coth\left(\frac{\beta eV}{2}\right) + \frac{2T^2(\varepsilon)}{\beta} \right\} \end{aligned} \quad (2)$$

and

$$\begin{aligned} A_{el}(V_d) &= \frac{e^3}{2\pi\hbar} \int d\varepsilon T(\varepsilon) [f_R(\varepsilon) - f_L(\varepsilon)] \\ &\quad + \frac{e^3}{2\pi\hbar} \int d\varepsilon \frac{3\Gamma_L^2 \Gamma_R^2 (f_R(\varepsilon) - f_L(\varepsilon)) (f_R(\varepsilon) + f_L(\varepsilon) - 2f_R(\varepsilon)f_L(\varepsilon))}{\left[(\varepsilon - \varepsilon_0(V_d))^2 + \frac{(\Gamma_L + \Gamma_R)^2}{4} \right]^2} \\ &\quad - \frac{e^3}{2\pi\hbar} \int d\varepsilon \frac{2\Gamma_L^3 \Gamma_R^3 [f_L(\varepsilon) - f_R(\varepsilon)]^3}{\left[(\varepsilon - \varepsilon_0(V_d))^2 + \frac{(\Gamma_L + \Gamma_R)^2}{4} \right]^3} \\ &= \frac{e^3}{h} \left\{ \text{Tr} [T(\varepsilon) (1-T^2(\varepsilon))] eV + \frac{3}{\beta} \text{Tr} [T^2(\varepsilon) (2-T(\varepsilon))] \right. \\ &\quad \left. + 3\text{Tr} [T^2(\varepsilon) (T(\varepsilon) - 1)] \coth\left(\frac{\beta eV}{2}\right) eV - \frac{1}{2\beta} \tanh^2\left(\frac{\beta eV}{2}\right) \text{Tr} [T^3(\varepsilon)] \right\} \end{aligned} \quad (3)$$

where $T(\varepsilon) = \frac{\Gamma_L \Gamma_R}{(\varepsilon - \varepsilon_0)^2 + (\Gamma_L + \Gamma_R)^2 / 4}$ is the transmission function,

$\varepsilon_0(V_d) = \varepsilon_0 + \frac{\Gamma_L - \Gamma_R}{\Gamma_L + \Gamma_R} V_d$ is the bias-dependent position of the single level, Γ_L (Γ_R) is the

level broadening due to the coupling to the left (right) lead, and $\bar{f}_{L/R}(\varepsilon) = 1 - f_{L/R}(\varepsilon)$,

$f_{L/R}(\varepsilon)$ is the Fermi distribution for left/right lead.

The inelastic corrections to the current cumulants due to the electron-phonon coupling could be explicitly divided into the mean-field corrections and the vertex corrections. In the low-transmission regime, corrections higher than $O(T(\varepsilon))$ were negligible and thus ignored for the third cumulant.

(iii) The Hartree terms for S and A are given by

$$A_H(V_d) = -\frac{e^4}{2\pi\hbar} \int \frac{4}{\hbar\omega} M_{eph}^2 N_e(\varepsilon) \frac{\Gamma_L \Gamma_R (f_L(\varepsilon, V_d) - f_R(\varepsilon, V_d))(\varepsilon - \varepsilon_0(V_d))}{\left[(\varepsilon - \varepsilon_0(V_d))^2 + \frac{(\Gamma_L + \Gamma_R)^2}{4} \right]^2} \quad (4)$$

$$S_H^{mf}(V_d) = -\frac{e^3}{2\pi\hbar} \int d\varepsilon \frac{4}{\hbar\omega} M_{eph}^2 N_e(\varepsilon) \frac{\Gamma_L \Gamma_R (f_L(\varepsilon, V_d) \bar{f}_R(\varepsilon, V_d) + f_R(\varepsilon, V_d) \bar{f}_L(\varepsilon, V_d))(\varepsilon - \varepsilon_0(V_d))}{\left[(\varepsilon - \varepsilon_0(V_d))^2 + \frac{(\Gamma_L + \Gamma_R)^2}{4} \right]^2} \\ + \frac{e^3}{2\pi\hbar} \int d\varepsilon \frac{8}{\hbar\omega} M_{eph}^2 N_e(\varepsilon) \frac{\Gamma_L^2 \Gamma_R^2 (f_L(\varepsilon, V_d) - f_R(\varepsilon, V_d))^2 (\varepsilon - \varepsilon_0(V_d))}{\left[(\varepsilon - \varepsilon_0(V_d))^2 + \frac{(\Gamma_L + \Gamma_R)^2}{4} \right]^3} \quad (5)$$

$$S_H^{vx}(V_d) = \frac{e^3}{2\pi\hbar} \int d\varepsilon i \frac{2}{\hbar\omega} M_{eph}^2 n_D^+(V_d) \frac{\Gamma_L \Gamma_R (f_L(\varepsilon, V_d) - f_R(\varepsilon, V_d))(\varepsilon - \varepsilon_0(V_d))}{\left[(\varepsilon - \varepsilon_0(V_d))^2 + \frac{(\Gamma_L + \Gamma_R)^2}{4} \right]^2} \\ + \frac{e^3}{2\pi\hbar} \int d\varepsilon \frac{2}{\hbar\omega} M_{eph}^2 n_D^-(V_d) \frac{\Gamma_L \Gamma_R (f_L(\varepsilon, V_d) - f_R(\varepsilon, V_d))}{\left[(\varepsilon - \varepsilon_0(V_d))^2 + \frac{(\Gamma_L + \Gamma_R)^2}{4} \right]^2} (\Gamma_L f_L(\varepsilon, V_d) + \Gamma_R f_R(\varepsilon, V_d) - (\Gamma_L + \Gamma_R)/2) \quad (6)$$

where

$$N_e(V_d) = \frac{1}{2\pi} \int d\varepsilon \frac{\Gamma_L f_L(\varepsilon, V_d) + \Gamma_R f_R(\varepsilon, V_d)}{(\varepsilon - \varepsilon_0(V_d))^2 + \frac{(\Gamma_L + \Gamma_R)^2}{4}} \quad (7)$$

$$n_D^-(V_d) = -\int d\varepsilon \frac{2\Gamma_L \Gamma_R (f_R(\varepsilon, V_d) \bar{f}_L(\varepsilon, V_d) - f_L(\varepsilon, V_d) \bar{f}_R(\varepsilon, V_d))(\varepsilon - \varepsilon_0(V_d))}{\left[(\varepsilon - \varepsilon_0(V_d))^2 + \frac{(\Gamma_L + \Gamma_R)^2}{4} \right]^2} \exp(-i0^+ \varepsilon / \hbar) \quad (8)$$

$$n_D^+(V_d) = \int d\varepsilon 2i \frac{\Gamma_L \Gamma_R (\Gamma_L f_L(\varepsilon, V_d) + \Gamma_R f_R(\varepsilon, V_d) - (\Gamma_L + \Gamma_R)/2)}{\left[(\varepsilon - \varepsilon_0(V_d))^2 + \frac{(\Gamma_L + \Gamma_R)^2}{4} \right]^2} \times \\ (f_R(\varepsilon, V_d) \bar{f}_L(\varepsilon, V_d) - f_L(\varepsilon, V_d) \bar{f}_R(\varepsilon, V_d)) \exp(-i0^+ \varepsilon / \hbar) \quad (9)$$

(iv) The Fock terms for S and A are given by

$$\begin{aligned}
A_F(V_d) = & -\frac{e^4}{2\pi\hbar} \int d\varepsilon \frac{\Gamma_L \Gamma_R (f_L(\varepsilon, V_d) - f_R(\varepsilon, V_d)) (\varepsilon - \varepsilon_0(V_d))}{\left[(\varepsilon - \varepsilon_0(V_d))^2 + \frac{(\Gamma_L + \Gamma_R)^2}{4} \right]^2} \Sigma_F^m(\varepsilon) \\
& -\frac{e^2}{2\pi\hbar} \int d\varepsilon i \frac{\Gamma_L \Gamma_R (\Gamma_L f_L(\varepsilon, V_d) + \Gamma_R f_R(\varepsilon, V_d) - (\Gamma_L + \Gamma_R)/2) (f_L(\varepsilon, V_d) - f_R(\varepsilon, V_d))}{\left[(\varepsilon - \varepsilon_0(V_d))^2 + \frac{(\Gamma_L + \Gamma_R)^2}{4} \right]^2} \Sigma_F^p(\varepsilon) \\
& + \frac{e^2}{2\pi\hbar} \int d\varepsilon i \frac{\Gamma_L f_L(\varepsilon, V_d)}{\left[(\varepsilon - \varepsilon_0(V_d))^2 + \frac{(\Gamma_L + \Gamma_R)^2}{4} \right]} (\Sigma_F^{+-} - \Sigma_F^{-+}) \\
& - \frac{e^2}{2\pi\hbar} \int d\varepsilon i \frac{\Gamma_L \Gamma_R (f_L(\varepsilon, V_d) - f_R(\varepsilon, V_d)) (\Gamma_L f_L(\varepsilon, V_d) + \Gamma_R f_R(\varepsilon, V_d))}{\left[(\varepsilon - \varepsilon_0(V_d))^2 + \frac{(\Gamma_L + \Gamma_R)^2}{4} \right]^2} (\Sigma_F^{+-} + \Sigma_F^{-+}) \\
& + \frac{e^2}{2\pi\hbar} \int d\varepsilon i \frac{\Gamma_L}{\left[(\varepsilon - \varepsilon_0(V_d))^2 + \frac{(\Gamma_L + \Gamma_R)^2}{4} \right]} \Sigma_F^{-+} \\
& + \frac{e^2}{2\pi\hbar} \int d\varepsilon i \frac{\Gamma_L \Gamma_R (f_L(\varepsilon, V_d) - f_R(\varepsilon, V_d)) (\Gamma_L + \Gamma_R)}{\left[(\varepsilon - \varepsilon_0(V_d))^2 + \frac{(\Gamma_L + \Gamma_R)^2}{4} \right]^2} \Sigma_F^{-+}
\end{aligned} \tag{10}$$

$$\begin{aligned}
S_F^{mf}(V_d) = & -\frac{e^3}{2\pi\hbar} \int d\varepsilon \frac{\Gamma_L \Gamma_R (f_L(\varepsilon, V_d) \bar{f}_R(\varepsilon, V_d) + f_R(\varepsilon, V_d) \bar{f}_L(\varepsilon, V_d)) (\varepsilon - \varepsilon_0(V_d))}{\left[(\varepsilon - \varepsilon_0(V_d))^2 + \frac{(\Gamma_L + \Gamma_R)^2}{4} \right]^2} \Sigma_F^m(\varepsilon) \\
& + \frac{e^3}{2\pi\hbar} \int d\varepsilon \frac{2\Gamma_L^2 \Gamma_R^2 (f_L(\varepsilon, V_d) - f_R(\varepsilon, V_d))^2 (\varepsilon - \varepsilon_0(V_d))}{\left[(\varepsilon - \varepsilon_0(V_d))^2 + \frac{(\Gamma_L + \Gamma_R)^2}{4} \right]^3} \Sigma_F^m(\varepsilon) \\
& + \frac{e^3}{2\pi\hbar} \int d\varepsilon i \frac{\Gamma_L \Gamma_R (f_L(\varepsilon, V_d) \bar{f}_R(\varepsilon, V_d) + f_R(\varepsilon, V_d) \bar{f}_L(\varepsilon, V_d)) (\Gamma_L f_L(\varepsilon, V_d) + \Gamma_R f_R(\varepsilon, V_d) - (\Gamma_L + \Gamma_R)/2)}{\left[(\varepsilon - \varepsilon_0(V_d))^2 + \frac{(\Gamma_L + \Gamma_R)^2}{4} \right]^2} \Sigma_F^p(\varepsilon) \\
& - \frac{e^3}{2\pi\hbar} \int d\varepsilon 2i \frac{\Gamma_L^2 \Gamma_R^2 (f_L(\varepsilon, V_d) - f_R(\varepsilon, V_d))^2 (\Gamma_L f_L(\varepsilon, V_d) + \Gamma_R f_R(\varepsilon, V_d) - (\Gamma_L + \Gamma_R)/2)}{\left[(\varepsilon - \varepsilon_0(V_d))^2 + \frac{(\Gamma_L + \Gamma_R)^2}{4} \right]^3} \Sigma_F^p(\varepsilon) \\
& - \frac{e^3}{2\pi\hbar} \int d\varepsilon i \frac{2\Gamma_L^2 \Gamma_R (f_L(\varepsilon, V_d) - f_R(\varepsilon, V_d)) f_L(\varepsilon, V_d)}{\left[(\varepsilon - \varepsilon_0(V_d))^2 + \frac{(\Gamma_L + \Gamma_R)^2}{4} \right]^2} (\Sigma_F^{+-}(\varepsilon) - \Sigma_F^{-+}(\varepsilon)) \\
& + \frac{e^3}{2\pi\hbar} \int d\varepsilon i \frac{\Gamma_L \Gamma_R (f_L(\varepsilon, V_d) \bar{f}_R(\varepsilon, V_d) + f_R(\varepsilon, V_d) \bar{f}_L(\varepsilon, V_d)) (\Gamma_L f_L(\varepsilon, V_d) + \Gamma_R f_R(\varepsilon, V_d))}{\left[(\varepsilon - \varepsilon_0(V_d))^2 + \frac{(\Gamma_L + \Gamma_R)^2}{4} \right]^2} (\Sigma_F^{+-}(\varepsilon) + \Sigma_F^{-+}(\varepsilon)) \\
& + \frac{e^3}{2\pi\hbar} \int d\varepsilon 2i \frac{\Gamma_L^2 \Gamma_R^2 (f_L(\varepsilon, V_d) - f_R(\varepsilon, V_d))^2 (\Gamma_L f_L(\varepsilon, V_d) + \Gamma_R f_R(\varepsilon, V_d))}{\left[(\varepsilon - \varepsilon_0(V_d))^2 + \frac{(\Gamma_L + \Gamma_R)^2}{4} \right]^3} (\Sigma_F^{+-}(\varepsilon) + \Sigma_F^{-+}(\varepsilon)) \\
& + \frac{e^3}{2\pi\hbar} \int d\varepsilon i \frac{\Gamma_L \Gamma_R (\Gamma_L + \Gamma_R) (f_L(\varepsilon, V_d) \bar{f}_R(\varepsilon, V_d) + f_R(\varepsilon, V_d) \bar{f}_L(\varepsilon, V_d))}{\left[(\varepsilon - \varepsilon_0(V_d))^2 + \frac{(\Gamma_L + \Gamma_R)^2}{4} \right]^2} \Sigma_F^{-+}(\varepsilon) \\
& - \frac{e^3}{2\pi\hbar} \int d\varepsilon 2i \frac{\Gamma_L^2 \Gamma_R^2 (\Gamma_L + \Gamma_R) (f_L(\varepsilon, V_d) - f_R(\varepsilon, V_d))^2}{\left[(\varepsilon - \varepsilon_0(V_d))^2 + \frac{(\Gamma_L + \Gamma_R)^2}{4} \right]^3} \Sigma_F^{-+}(\varepsilon) \\
& - \frac{e^2}{2\pi\hbar} \int d\varepsilon i \frac{2\Gamma_L^2 \Gamma_R (f_L(\varepsilon, V_d) - f_R(\varepsilon, V_d))}{\left[(\varepsilon - \varepsilon_0(V_d))^2 + \frac{(\Gamma_L + \Gamma_R)^2}{4} \right]^2} \Sigma_F^{-+}(\varepsilon) \\
& - \frac{e^2}{2\pi\hbar} \int d\varepsilon i \frac{\Gamma_L}{\left[(\varepsilon - \varepsilon_0(V_d))^2 + \frac{(\Gamma_L + \Gamma_R)^2}{4} \right]} \Sigma_F^{+-}(\varepsilon)
\end{aligned} \tag{11}$$

$$\begin{aligned}
S_F^{\text{vx}}(V_d) = & \frac{e^3}{2\pi\hbar} \int d\varepsilon i \frac{\Gamma_L \Gamma_R (f_L(\varepsilon, V_d) - f_R(\varepsilon, V_d)) (\varepsilon - \varepsilon_0(V_d))}{\left[(\varepsilon - \varepsilon_0(V_d))^2 + \frac{(\Gamma_L + \Gamma_R)^2}{4} \right]^2} \Sigma_{F,D}^{+++,m,--}(\varepsilon) \\
& + \frac{e^3}{2\pi\hbar} \int d\varepsilon \frac{\Gamma_L f_L(\varepsilon, V_d) \Sigma_{F,D}^{+-,m,+}(\varepsilon) + \Gamma_L \Sigma_{F,D}^{-+}(\varepsilon)}{\left[(\varepsilon - \varepsilon_0(V_d))^2 + \frac{(\Gamma_L + \Gamma_R)^2}{4} \right]} \\
& + \frac{e^3}{2\pi\hbar} \int d\varepsilon \frac{\Gamma_L \Gamma_R (\Gamma_L f_L(\varepsilon, V_d) + \Gamma_R f_R(\varepsilon, V_d) - (\Gamma_L + \Gamma_R)/2) (f_L(\varepsilon, V_d) - f_R(\varepsilon, V_d))}{\left[(\varepsilon - \varepsilon_0(V_d))^2 + \frac{(\Gamma_L + \Gamma_R)^2}{4} \right]^2} \Sigma_{F,D}^{+++,p,--}(\varepsilon) \\
& - \frac{e^3}{2\pi\hbar} \int d\varepsilon \frac{\Gamma_L \Gamma_R (\Gamma_L f_L(\varepsilon, V_d) + \Gamma_R f_R(\varepsilon, V_d)) (f_L(\varepsilon, V_d) - f_R(\varepsilon, V_d))}{\left[(\varepsilon - \varepsilon_0(V_d))^2 + \frac{(\Gamma_L + \Gamma_R)^2}{4} \right]^2} \Sigma_{F,D}^{+-,p,+}(\varepsilon) \\
& + \frac{e^3}{2\pi\hbar} \int d\varepsilon \frac{\Gamma_L \Gamma_R (\Gamma_L + \Gamma_R) (f_L(\varepsilon, V_d) - f_R(\varepsilon, V_d))}{\left[(\varepsilon - \varepsilon_0(V_d))^2 + \frac{(\Gamma_L + \Gamma_R)^2}{4} \right]^2} \Sigma_{F,D}^{-+}(\varepsilon)
\end{aligned} \tag{12}$$

where

$$\begin{aligned}
\Sigma_F^p(\varepsilon) = & iM_{e-ph}^2 (2N_p + 1) \frac{\Gamma_L (f_L(\varepsilon + \hbar\omega, V_d) + f_L(\varepsilon - \hbar\omega, V_d) - 1) + \Gamma_R (f_R(\varepsilon + \hbar\omega, V_d) + f_R(\varepsilon - \hbar\omega, V_d) - 1)}{\left[(\varepsilon - \varepsilon_0(V_d))^2 + \frac{(\Gamma_L + \Gamma_R)^2}{4} \right]} \\
& - iM_{e-ph}^2 \frac{\text{Im}(\mathbf{g}^r(\varepsilon + \hbar\omega, V_d) - \mathbf{g}^r(\varepsilon - \hbar\omega, V_d))}{\left[(\varepsilon - \varepsilon_0(V_d))^2 + \frac{(\Gamma_L + \Gamma_R)^2}{4} \right]}
\end{aligned} \tag{13}$$

$$\begin{aligned}
\Sigma_F^m(\varepsilon) = & -2M_{e-ph}^2 (2N_p + 1) \text{Re}[\mathbf{g}^r(\varepsilon, V_d)] \\
& - M_{e-ph}^2 (\text{Re}[\mathbf{g}^r(\varepsilon - \hbar\omega, V_d)] - \text{Re}[\mathbf{g}^r(\varepsilon + \hbar\omega, V_d)]) \\
& + iM_{e-ph}^2 \left(\text{Hilb}\left(\mathbf{g}^{++}(\varepsilon, V_d), \frac{1}{\varepsilon - \hbar\omega}\right) - \text{Hilb}\left(\mathbf{g}^{++}(\varepsilon, V_d), \frac{1}{\varepsilon + \hbar\omega}\right) \right)
\end{aligned} \tag{14}$$

$$\Sigma_F^{+-}(\varepsilon) = M_{e-ph}^2 \left((N_p + 1) \mathbf{g}^{+-}(\varepsilon + \hbar\omega, V_d) + N_p \mathbf{g}^{+-}(\varepsilon - \hbar\omega, V_d) \right) \tag{15}$$

$$\Sigma_F^{+-}(\varepsilon) = M_{e-ph}^2 \left((N_p + 1) \mathbf{g}^{+-}(\varepsilon - \hbar\omega, V_d) + N_p \mathbf{g}^{+-}(\varepsilon + \hbar\omega, V_d) \right) \tag{16}$$

$$\begin{aligned}
\Sigma_{F,D}^{++p,-}(\varepsilon) = & -M_{e-ph}^2 (2N_p + 1) \frac{\Gamma_L \Gamma_R}{\left[(\varepsilon - \varepsilon_0(V_d))^2 + \frac{(\Gamma_L + \Gamma_R)^2}{4} \right]^2} \{ \\
& (\Gamma_L f_L(\varepsilon + \hbar\omega, V_d) + \Gamma_R f_R(\varepsilon + \hbar\omega, V_d) - (\Gamma_L + \Gamma_R)/2) \times \\
& (f_R(\varepsilon + \hbar\omega, V_d) \bar{f}_L(\varepsilon + \hbar\omega, V_d) - f_L(\varepsilon + \hbar\omega, V_d) \bar{f}_R(\varepsilon + \hbar\omega, V_d)) \\
& + (\Gamma_L f_L(\varepsilon - \hbar\omega, V_d) + \Gamma_R f_R(\varepsilon - \hbar\omega, V_d) - (\Gamma_L + \Gamma_R)/2) \times \\
& (f_R(\varepsilon - \hbar\omega, V_d) \bar{f}_L(\varepsilon - \hbar\omega, V_d) - f_L(\varepsilon - \hbar\omega, V_d) \bar{f}_R(\varepsilon - \hbar\omega, V_d)) \} \\
& + iM_{eph}^2 \left(\text{Hilb} \left(\text{CauP}_1(\varepsilon, V_d), \frac{1}{\varepsilon - \hbar\omega} \right) - \text{Hilb} \left(\text{CauP}_1(\varepsilon, V_d), \frac{1}{\varepsilon + \hbar\omega} \right) \right) \quad (17)
\end{aligned}$$

$$\text{CauP}_1(\varepsilon, V_d) = -i \frac{2\Gamma_L \Gamma_R (f_R(\varepsilon, V_d) \bar{f}_L(\varepsilon, V_d) - f_L(\varepsilon, V_d) \bar{f}_R(\varepsilon, V_d)) (\varepsilon - \varepsilon_0(V_d))}{\left[(\varepsilon - \varepsilon_0(V_d))^2 + \frac{(\Gamma_L + \Gamma_R)^2}{4} \right]^2} \quad (18)$$

$$\begin{aligned}
\Sigma_{F,D}^{++m,-}(\varepsilon) = & -iM_{e-ph}^2 (2N_p + 1) \frac{\Gamma_L \Gamma_R}{\left[(\varepsilon - \varepsilon_0(V_d))^2 + \frac{(\Gamma_L + \Gamma_R)^2}{4} \right]^2} \{ \\
& (\varepsilon + \hbar\omega - \varepsilon_0(V_d)) (f_R(\varepsilon + \hbar\omega, V_d) \bar{f}_L(\varepsilon + \hbar\omega, V_d) - f_L(\varepsilon + \hbar\omega, V_d) \bar{f}_R(\varepsilon + \hbar\omega, V_d)) \\
& + (\varepsilon - \hbar\omega - \varepsilon_0(V_d)) (f_R(\varepsilon - \hbar\omega, V_d) \bar{f}_L(\varepsilon - \hbar\omega, V_d) - f_L(\varepsilon - \hbar\omega, V_d) \bar{f}_R(\varepsilon - \hbar\omega, V_d)) \} \\
& + iM_{eph}^2 \left(\text{Hilb} \left(\text{CauP}_2(\varepsilon, V_d), \frac{1}{\varepsilon - \hbar\omega} \right) - \text{Hilb} \left(\text{CauP}_2(\varepsilon, V_d), \frac{1}{\varepsilon + \hbar\omega} \right) \right) \quad (19)
\end{aligned}$$

$$\text{CauP}_2(\varepsilon, V_d) = - \frac{2\Gamma_L \Gamma_R (\Gamma_L f_L(\varepsilon, V_d) + \Gamma_R f_R(\varepsilon, V_d) - (\Gamma_L + \Gamma_R)/2) (f_R(\varepsilon, V_d) \bar{f}_L(\varepsilon, V_d) - f_L(\varepsilon, V_d) \bar{f}_R(\varepsilon, V_d))}{\left[(\varepsilon - \varepsilon_0(V_d))^2 + \frac{(\Gamma_L + \Gamma_R)^2}{4} \right]^2} \quad (20)$$

$$\begin{aligned}
\Sigma_{F,D}^{+-,m,-+}(\varepsilon) = & -M_{e-ph}^2 N_p \left[\frac{\Gamma_L}{(\varepsilon - \varepsilon_0(V_d))^2 + \frac{(\Gamma_L + \Gamma_R)^2}{4}} \right] \left(\bar{f}_L(\varepsilon + \hbar\omega, V_d) - f_L(\varepsilon + \hbar\omega, V_d) + \bar{f}_L(\varepsilon - \hbar\omega, V_d) - f_L(\varepsilon - \hbar\omega, V_d) \right) \\
& + M_{e-ph}^2 N_p \frac{\Gamma_L \Gamma_R (\Gamma_L + \Gamma_R)}{\left[(\varepsilon - \varepsilon_0(V_d))^2 + \frac{(\Gamma_L + \Gamma_R)^2}{4} \right]^2} \left\{ f_R(\varepsilon + \hbar\omega, V_d) \bar{f}_L(\varepsilon + \hbar\omega, V_d) - f_L(\varepsilon + \hbar\omega, V_d) \bar{f}_R(\varepsilon + \hbar\omega, V_d) \right. \\
& + f_R(\varepsilon - \hbar\omega, V_d) \bar{f}_L(\varepsilon - \hbar\omega, V_d) - f_L(\varepsilon - \hbar\omega, V_d) \bar{f}_R(\varepsilon - \hbar\omega, V_d) \left. \right\} \\
& + \left(\Gamma_L f_L(\varepsilon - \hbar\omega, V_d) + \Gamma_R f_R(\varepsilon - \hbar\omega, V_d) - (\Gamma_L + \Gamma_R)/2 \right) \times \\
& \left(f_R(\varepsilon - \hbar\omega, V_d) \bar{f}_L(\varepsilon - \hbar\omega, V_d) - f_L(\varepsilon - \hbar\omega, V_d) \bar{f}_R(\varepsilon - \hbar\omega, V_d) \right) \left. \right\} \\
& + M_{e-ph}^2 \left[\frac{\Gamma_L}{(\varepsilon - \varepsilon_0(V_d))^2 + \frac{(\Gamma_L + \Gamma_R)^2}{4}} \right] \left(f_L(\varepsilon + \hbar\omega, V_d) - f_L(\varepsilon - \hbar\omega, V_d) \right) \\
& + M_{e-ph}^2 \frac{\Gamma_L \Gamma_R}{\left[(\varepsilon - \varepsilon_0(V_d))^2 + \frac{(\Gamma_L + \Gamma_R)^2}{4} \right]^2} \left(\Gamma_L f_L(\varepsilon, V_d) + \Gamma_R f_R(\varepsilon, V_d) \right) \left\{ \right. \\
& f_R(\varepsilon + \hbar\omega, V_d) \bar{f}_L(\varepsilon + \hbar\omega, V_d) - f_L(\varepsilon + \hbar\omega, V_d) \bar{f}_R(\varepsilon + \hbar\omega, V_d) \left. \right\} \\
& + M_{e-ph}^2 \frac{\Gamma_L \Gamma_R}{\left[(\varepsilon - \varepsilon_0(V_d))^2 + \frac{(\Gamma_L + \Gamma_R)^2}{4} \right]^2} \left(\Gamma_L \bar{f}_L(\varepsilon, V_d) + \Gamma_R \bar{f}_R(\varepsilon, V_d) \right) \left\{ \right. \\
& f_R(\varepsilon - \hbar\omega, V_d) \bar{f}_L(\varepsilon - \hbar\omega, V_d) - f_L(\varepsilon - \hbar\omega, V_d) \bar{f}_R(\varepsilon - \hbar\omega, V_d) \left. \right\}
\end{aligned} \tag{21}$$

$$\begin{aligned}
\Sigma_{F,D}^{+-,p,-+}(\varepsilon) = & -M_{e-ph}^2 N_p \left[\frac{\Gamma_L}{(\varepsilon - \varepsilon_0(V_d))^2 + \frac{(\Gamma_L + \Gamma_R)^2}{4}} \right] \\
& + M_{e-ph}^2 N_p \frac{\Gamma_L \Gamma_R}{\left[(\varepsilon - \varepsilon_0(V_d))^2 + \frac{(\Gamma_L + \Gamma_R)^2}{4} \right]^2} \left\{ \left[\Gamma_L (\bar{f}_L(\varepsilon + \hbar\omega, V_d) - f_L(\varepsilon + \hbar\omega, V_d)) \right. \right. \\
& + \Gamma_R (\bar{f}_R(\varepsilon + \hbar\omega, V_d) - f_R(\varepsilon + \hbar\omega, V_d)) \left. \right] (f_R(\varepsilon + \hbar\omega, V_d) \bar{f}_L(\varepsilon + \hbar\omega, V_d) - f_L(\varepsilon + \hbar\omega, V_d) \bar{f}_R(\varepsilon + \hbar\omega, V_d)) \\
& + \left[\Gamma_L (\bar{f}_L(\varepsilon - \hbar\omega, V_d) - f_L(\varepsilon - \hbar\omega, V_d)) + \Gamma_R (\bar{f}_R(\varepsilon - \hbar\omega, V_d) - f_R(\varepsilon - \hbar\omega, V_d)) \right] \times \\
& (f_R(\varepsilon - \hbar\omega, V_d) \bar{f}_L(\varepsilon - \hbar\omega, V_d) - f_L(\varepsilon - \hbar\omega, V_d) \bar{f}_R(\varepsilon - \hbar\omega, V_d)) \left. \right\} \\
& - M_{e-ph}^2 \left[\frac{\Gamma_L}{(\varepsilon - \varepsilon_0(V_d))^2 + \frac{(\Gamma_L + \Gamma_R)^2}{4}} \right] f_L(\varepsilon + \hbar\omega, V_d) \\
& - M_{e-ph}^2 \frac{\Gamma_L \Gamma_R}{\left[(\varepsilon - \varepsilon_0(V_d))^2 + \frac{(\Gamma_L + \Gamma_R)^2}{4} \right]^2} (\Gamma_L f_L(\varepsilon + \hbar\omega, V_d) + \Gamma_R f_R(\varepsilon + \hbar\omega, V_d)) \times \\
& f_R(\varepsilon + \hbar\omega, V_d) \bar{f}_L(\varepsilon + \hbar\omega, V_d) - f_L(\varepsilon + \hbar\omega, V_d) \bar{f}_R(\varepsilon + \hbar\omega, V_d) \\
& - M_{e-ph}^2 \left[\frac{\Gamma_L}{(\varepsilon - \varepsilon_0(V_d))^2 + \frac{(\Gamma_L + \Gamma_R)^2}{4}} \right] \bar{f}_L(\varepsilon - \hbar\omega, V_d) \\
& - M_{e-ph}^2 \frac{\Gamma_L \Gamma_R}{\left[(\varepsilon - \varepsilon_0(V_d))^2 + \frac{(\Gamma_L + \Gamma_R)^2}{4} \right]^2} (\Gamma_L \bar{f}_L(\varepsilon - \hbar\omega, V_d) + \Gamma_R \bar{f}_R(\varepsilon - \hbar\omega, V_d)) \times \\
& (f_R(\varepsilon - \hbar\omega, V_d) \bar{f}_L(\varepsilon - \hbar\omega, V_d) - f_L(\varepsilon - \hbar\omega, V_d) \bar{f}_R(\varepsilon - \hbar\omega, V_d)) \tag{22}
\end{aligned}$$

$$\begin{aligned}
\Sigma_{F,D}^{-+}(\varepsilon) = & -M_{e-ph}^2 (N_p + 1) \left[\frac{\Gamma_L}{(\varepsilon - \varepsilon_0(V_d))^2 + \frac{(\Gamma_L + \Gamma_R)^2}{4}} \right] f_L(\varepsilon + \hbar\omega, V_d) \\
& - M_{e-ph}^2 N_p \left[\frac{\Gamma_L}{(\varepsilon - \varepsilon_0(V_d))^2 + \frac{(\Gamma_L + \Gamma_R)^2}{4}} \right] f_L(\varepsilon - \hbar\omega, V_d) \\
& - M_{e-ph}^2 (N_p + 1) \frac{\Gamma_L \Gamma_R}{\left[(\varepsilon - \varepsilon_0(V_d))^2 + \frac{(\Gamma_L + \Gamma_R)^2}{4} \right]^2} (\Gamma_L f_L(\varepsilon + \hbar\omega, V_d) + \Gamma_R f_R(\varepsilon + \hbar\omega, V_d)) \times \\
& (f_R(\varepsilon + \hbar\omega, V_d) \bar{f}_L(\varepsilon + \hbar\omega, V_d) - f_L(\varepsilon + \hbar\omega, V_d) \bar{f}_R(\varepsilon + \hbar\omega, V_d)) \\
& - M_{e-ph}^2 N_p \frac{\Gamma_L \Gamma_R}{\left[(\varepsilon - \varepsilon_0(V_d))^2 + \frac{(\Gamma_L + \Gamma_R)^2}{4} \right]^2} (\Gamma_L f_L(\varepsilon - \hbar\omega, V_d) + \Gamma_R f_R(\varepsilon - \hbar\omega, V_d)) \times \\
& (f_R(\varepsilon - \hbar\omega, V_d) \bar{f}_L(\varepsilon - \hbar\omega, V_d) - f_L(\varepsilon - \hbar\omega, V_d) \bar{f}_R(\varepsilon - \hbar\omega, V_d)) \tag{23}
\end{aligned}$$

Here, $\text{Tr}[\dots]$ is the trace operation and $\text{Hilb}(\dots)$ stands for the Hilbert transform, M_{e-ph} is the electron-phonon coupling constant, N_p is the thermal expectation value of the phonon occupation, $g^{r/a/+/-+}(\varepsilon)$ is the free retarded/advanced/greater/lesser Green's function of the single level.

(v) Numerical calculations

The calculation results for the skewness are very robust. The peak positions of the skewness in the Γ - M_{e-ph} map and the ε_0 - M_{e-ph} map at different vibration frequencies ($\hbar\omega = 25$ meV, 50 meV and 75 meV) are shown in Fig. S12 and Fig. S13, respectively.

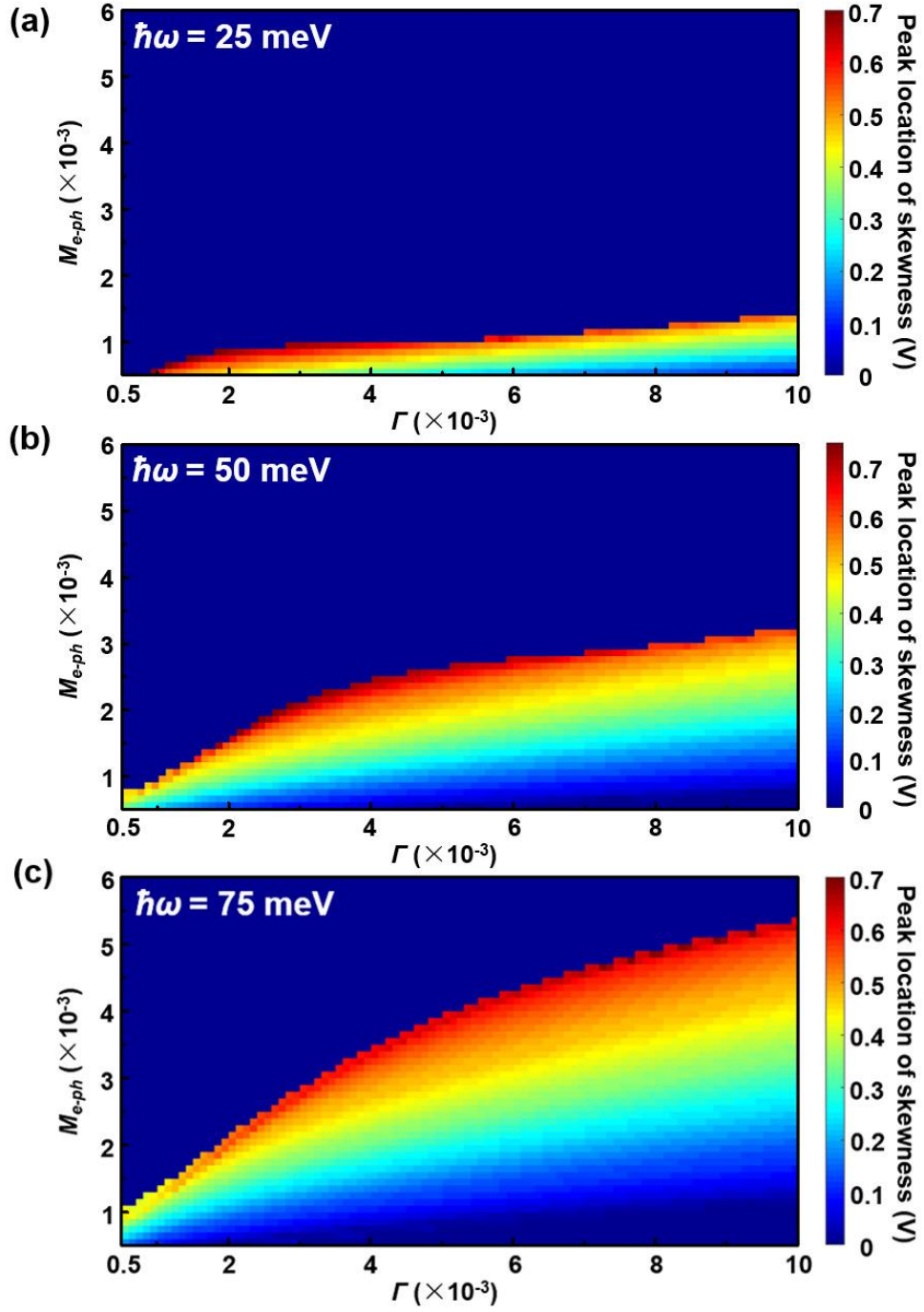


Figure S12. The peak positions of the skewness in the Γ - M_{e-ph} map at different vibration frequencies. (a) $\hbar\omega = 25$ meV, (b) $\hbar\omega = 50$ meV and (c) $\hbar\omega = 75$ meV. ε_0 was set at -0.42 eV. The peaks were ignored when their values were less than 0.01.

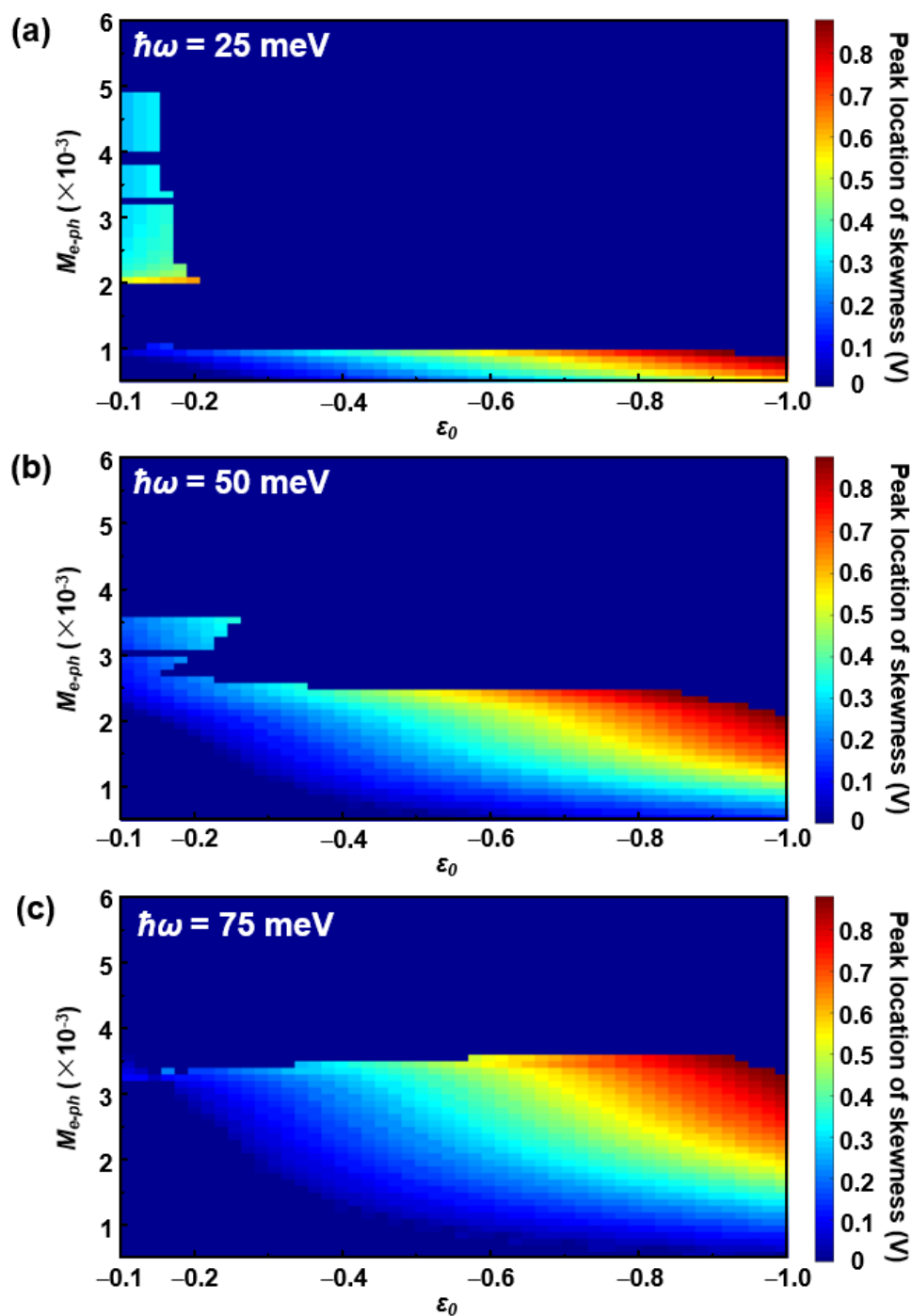


Figure S13. The peak positions of the skewness in the ε_0 – M_{e-ph} map at different vibration frequencies. (a) $\hbar\omega = 25$ meV, (b) $\hbar\omega = 50$ meV and (c) $\hbar\omega = 75$ meV. Γ was set at 4.2 meV. The peaks were ignored when their values were less than 0.01.

8. References:

1. Y. Cao, S. Dong, S. Liu, L. He, L. Gan, X. Yu, M. L. Steigerwald, X. Wu, Z. Liu and X. Guo. *Angew. Chem., Int. Ed.* 2012, **51**, 12228